International Journal of Engineering Inventions
e-ISSN: 2278-7461, p-ISSN: 2319-6491
Volume 14, Issue 5 [May. 2025] PP: 48-52

Study on the Production of High-Manganese Steel Powder by Mechanical Milling Method

Hoang Anh Quang, Ha Bach Tu
Mechanical Engineering Faculty, Thai Nguyen University of Technology, Thai Nguyen, Vietnam

Abstract
High-manganese steel powder was fabricated by mechanical milling from manganese steel chips for use as the matrix material in metal matrix composites (MMCs). The steel chips were milled using a planetary ball mill at speeds from 300 to 450 rpm for 4 to 20 hours in a hexane medium. The resulting crystalline structure and phase composition were analyzed via X-ray diffraction (XRD). Microstructure, surface morphology, and particle size of the milled powder were examined using scanning electron microscopy (SEM) and laser diffraction particle size analysis. Through the study of milling parameters (speed, duration), the final powder achieved the desired FeMn phase composition with fine particle size suitable for composite applications.
Keywords: *manganese steel, steel powder, mechanical milling*

Date of Submission: 28-04-2025 Date of acceptance: 07-05-2025

I. Introduction

Metal matrix composites (MMCs) have been studied, developed, and applied in many industries such as cutting tools, grinding tools, aerospace, and automotive sectors due to their low cost and excellent mechanical properties. MMCs often use ceramic reinforcements (e.g., TiC, SiC, TiB_2 , $Al_2 O_3$, B_4 C, WC, VC) combined with a tough metal or alloy matrix to create materials with high hardness (wear resistance), toughness (impact resistance), and strength (load-bearing capability).

High-manganese steel is an alloy steel containing a high Mn content (>10%) and is widely used in mining, stone, cement, and mineral processing due to its excellent mechanical properties and chemical stability [12]. After heat treatment, it exhibits an austenitic structure with high toughness and wear resistance under impact conditions due to its work-hardening capability [21]. Manganese contents above 14% result in improved wear resistance. However, wear resistance of steels with Mn <14% has also been improved with ceramic particle reinforcement [17,18]. Therefore, to enhance service life, wear resistance, and mechanical properties, steel matrix composites with ceramic reinforcements have been developed [10,19]. The combination of hard TiC particles with a high-Mn austenitic steel matrix significantly improves wear resistance [1,23].

Composite fabrication technologies include solid-state synthesis and melt casting [15,9,6]. Solid-state synthesis methods include powder metallurgy, self-propagating high-temperature synthesis (SHS), mechanical alloying, and carbothermal reduction [16,20,4,7,2,3,13,22,8]. Melt casting offers advantages such as low cost, scalability, and the ability to produce large and complex parts, but it requires high temperatures and may lead to segregation during solidification [19,14]. Powder metallurgy is simple and suitable for producing composites with a high ceramic content, precise control, stable and uniform particle distribution, and minimal material loss, making it widely used for metal matrix composite production.

Powder production methods include physical (atomization), chemical (oxide reduction), electrolysis, and mechanical (milling). This paper focuses on producing high-manganese steel powder for use as a composite matrix using mechanical milling of steel chips.

II. Experimental Procedure

In this study, high-manganese steel powder was produced from manganese steel chips with the chemical composition shown in Table 1.

Table 1. Chemical composition of the steel chips

Element	C	Si	Mn	P	S	Cr	Mo	Ni	Cu	Fe
%	0,962	0,399	13,421	0,041	0,011	2,202	0,062	0,399	0,201	82,364

The powder production process is illustrated in Figure 1. Steel chips with dimensions of 0.2×5×30 mm were coarse-milled using a drum mill (drum size 200×350 mm) for 2 hours at 150 rpm with a ball-to-chip weight ratio of 8:1 in a hexane medium. After coarse milling, the powder was sieved to obtain particles smaller than 200 μm and then further refined using a planetary ball mill under different milling regimes.

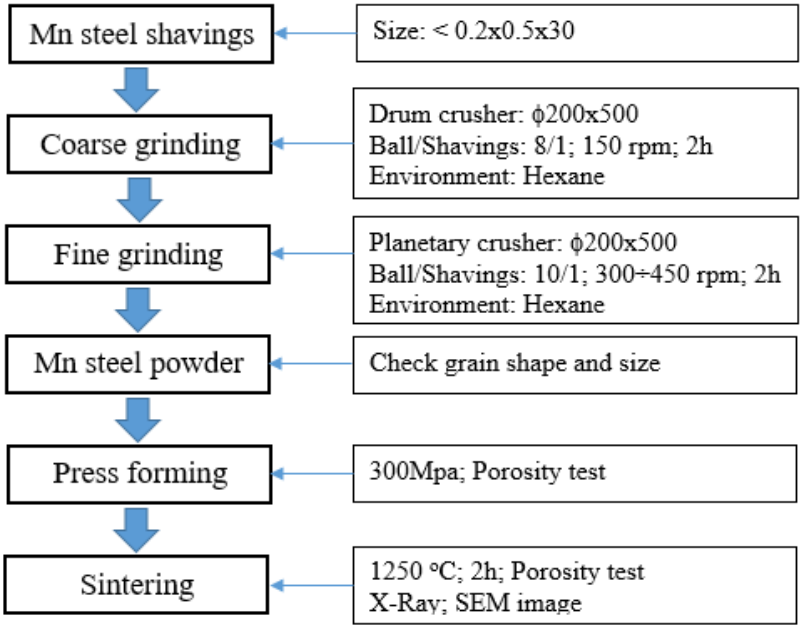

Figure 1. Process flowchart for high-manganese steel powder production

Fine powder (M1) was compacted in a steel mold at 300 MPa. Porosity was measured by hydrostatic weighing based on Archimedes' principle to evaluate powder compressibility.

The compacted M1 powder was sintered at 1250°C for 2 hours in an argon atmosphere to analyze microstructure, sinterability, and phase composition. Commercial powder (M2) was also compacted and sintered under the same conditions for comparison.

The average particle size was measured by laser diffraction analysis. Powder morphology was observed via scanning electron microscopy (SEM, Cambridge LEO-1450). Phase composition was determined by X-ray diffraction (XRD, D8 ADVANCE).

III. Results and Discussion

3.1. Effect of Milling Parameters on Particle Size

To investigate the effect of milling parameters on Mn steel powder particle size, the coarse-milled steel chips (<200 µm) were further milled at speeds ranging from 300 to 450 rpm for durations from 0 to 20 hours. The resulting particle size varied with speed and duration, as shown in Figure 2.

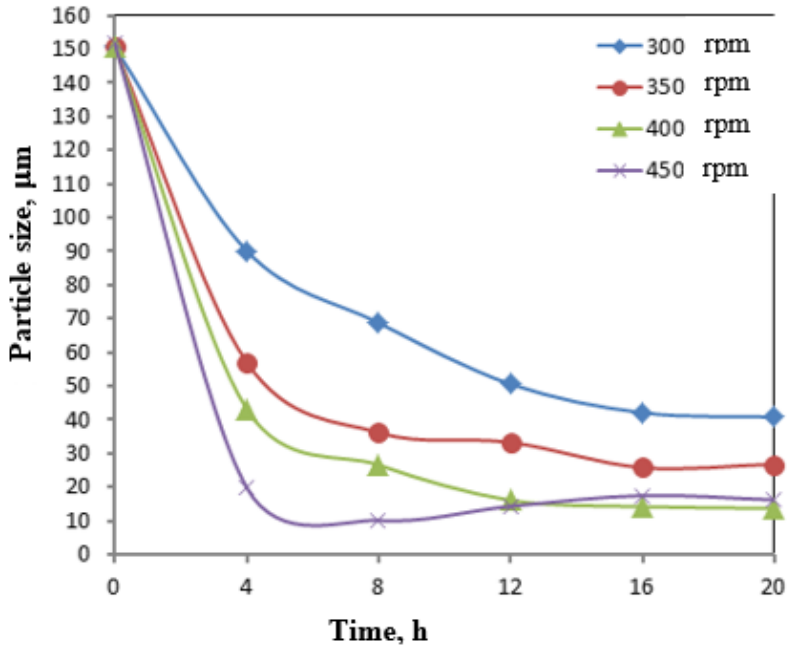

Figure 2. Effect of milling time on particle size

From figure 2 shows: During the initial 4 hours, particle size decreased rapidly, then more gradually between 4–8 hours. Initially, large particles and a high collision rate between balls and particles caused rapid size reduction. As particle size decreased, cold welding and reduced collision energy slowed further size reduction.
At each milling speed, particle size approached a minimum limit and then stabilized. Smaller particles increased the system's free energy due to higher surface energy, promoting cold welding, which in turn counteracts further fragmentation.
High grinding speed (large grinding energy), particle size decreases faster. Grinding efficiency increases rapidly when speed increases from 300 to 400 rpm. At 450 rpm, if grinding time is extended, the powder particle size increases, the cause may be due to high grinding energy heating the grinding mixture, promoting the cold welding process.

3.2. Effect of Milling on Powder Compressibility
Powder compressibility was evaluated through density or porosity after compaction. At a pressure of 300 MPa, porosity of the samples is shown in Figure 3.

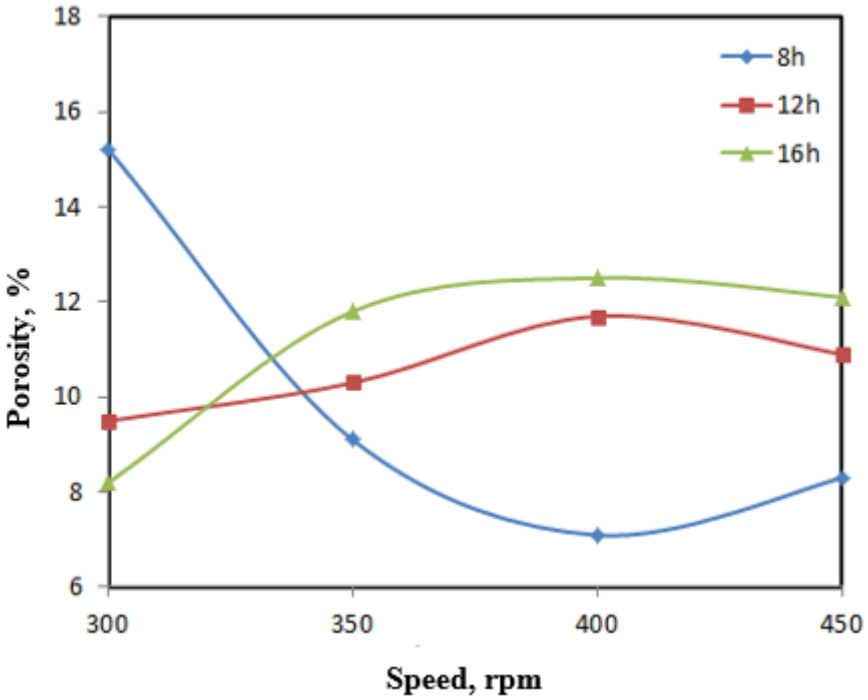

Figure 3. Effect of milling speed on porosity

With prolonged milling (12h, 16h), porosity increased as milling speed increased. For 8-hour milling, porosity decreased with increasing speed from 300 to 400 rpm, và porosity increased at 450 rpm due to work hardening of particles, which resisted compaction. To minimize porosity, excessive milling duration and speed should be avoided. The lowest porosity (7.1%) was achieved at 400 rpm for 8 hours.

3.3. Effect of Milling on Particle Morphology and Sinterability
SEM images of milled powder (M1) are shown in Figure 4(a). Ball collisions flattened particles, increasing surface area and enhancing inter-particle contact, which facilitated sintering.
Sintered samples exhibited strong bonding (Figure 5a) with low porosity (2.7%). In contrast, commercial powder (M2) with coarser particles (~150 µm, Figure 4b) showed poor bonding and higher porosity (11.9%) after sintering (Figure 5b).
XRD analysis (Figure 6) of sintered M1 showed phases of Fe(Mn) solid solution and $(FeMn)_3$ C carbides, consistent with the Fe–C–Mn phase diagram. No oxidation or foreign phases were detected during milling, compaction, or sintering.

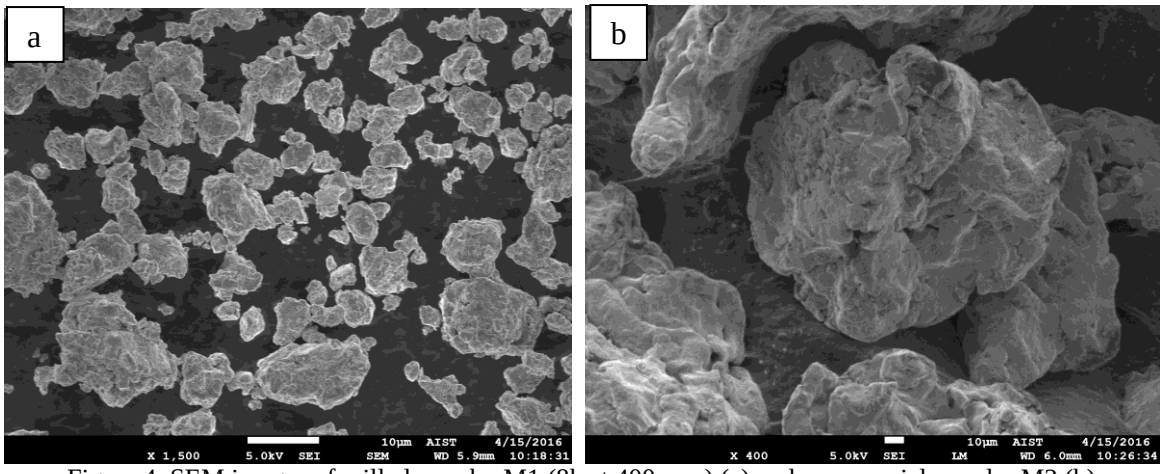

Figure 4. SEM images of milled powder M1 (8h at 400 rpm) (a) and commercial powder M2 (b)

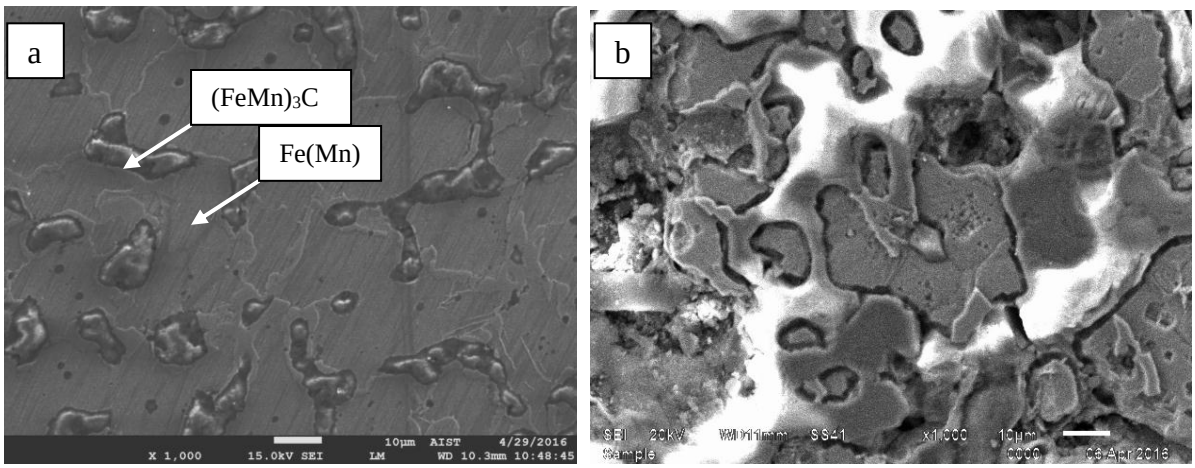

Figure 5. SEM images of sintered samples (1250°C, 2h) - M1 (a) and M2 (b)

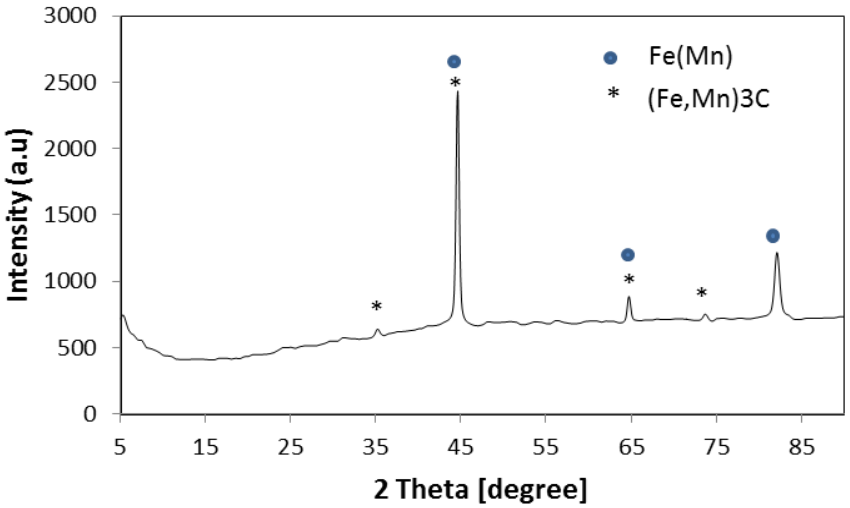

Figure 6. XRD of sintered M1 powder (1250°C, 2h)

IV. Conclusion

High-manganese steel powder for use as the matrix in TiC/Mn steel composites was successfully produced via mechanical milling. Under optimal milling conditions (400 rpm, 8 hours), the resulting powder had an average particle size of 26.6 µm, good compressibility, and excellent sinterability (porosity of 2.7%). The phase composition aligned with theoretical expectations, confirming its suitability as a composite matrix material.

References

[1]. Ashok Kumar Srivastava and Karabi Das (2009). In-situ Synthesis and Characterization of TiC reinforced Hadfield Manganese Austenitic Steel Matrix Composite. *ISIJ International*, Vol. 49, No. 9, pp. 1372–1377.

[2]. B.H. Li, Y. Liu, J. Li, H. Cao and L. He (2010). Effect of process on the microstructures and the properties of in situ TiB2-TiC reinforces steel matrix composites produced by spark plasma sintering. *J. Mater. Process. Technol*, 210, pp. 91-95.

[3]. C.L. Han and M.G. Kong (2009). Fabrication and properties of TiC-based cermet with intra/intergranular microstructure. *Mater. Des*, 30, pp. 1205-1208.

[4]. D.H. Bacon, L. Edwards, J.E. Moffatt and M.E. Fitzpatrick (2013). Fatigue and fracture of a 316 stainless steel metal matrix composite reinforced with 25% titanium diboride. *Int. J. Fatigue*, 48, pp. 39-47.

[5]. E. Pagounis, M. Talvitie and V.K. Lindroos (1996). Influence of the metal/cermet interface on the microstructure and mechanical properties of HIPed iron-based composites. *Compos. Sci. Technol*, 56, pp. 1329-1930.

[6]. F. Akhtar, S.J. Askari, J.A. Shah and S.J. Guo (2007). Processing, microstructure and mechanical properties of TiC-465 stainless steel/465 stainless steel layer composites. *J. Alloys Compd*, 493, pp. 287-293.

[7]. F. Akhtar and S.J. Guo (208). Microstructure, mechanical and fretting wear properties of TiC-stainless steel composites. *Mater. Charact*, 59, pp. 84-90.

[8]. H. Kwon, C.Y. Suh and W. Kim (2015). Microstructure and mechanical properties of (TiW)C-Ni cermet prepared using a nano-sized TiC-WC powder mixture. *J. Alloys Compd*, 639, pp. 21-26.

[9]. J.J. Park, S.M. Hong, M.K. Lee and C.K. Rhee (2013). Effects of metal additions on refinement behavior of TiC particles during a very high speed milling process. *Powder Technol*, 249, pp. 126-133.

[10]. K. I. Parshivamurthy, R. K. Kumar, S. Seetharamu and M. N. Chandrasekharaiah (2001). Review on TiC reinforced steel composites. *J. Mater. Sci*, Vol 36, pp. 4519-4530.

[11]. K.S. Ashok and D. Karabi (2008). Microstructure and abrasive wear study of (TiW)C reinforced high-manganese austenitic steel matrix composite. *Mater. Lett*, 62, pp. 3947-3950.

[12]. M.O. Hugo, E. Peter and K. Hans (2014). The history of the technology process of hardmetals. *Int. J. Refract. Met. Hard Mater*, 44, pp. 148-159.

[13]. O.R. Wiedemanm, C. Weck, U. Martin, A. Muller and H.J. Seifert (2012). Spark plasma sintering of TiC particle-reinforced molybdenum composites. *Int. J. Refract. Met. Hard Mater*, 32, pp. 1-6.

[14]. Ö.N. Dog˘an, J.A. Hawk, and K.K. Schrems (2006). TiC-Reinforced Cast Cr Steels. *JMEPEG*, 15, pp. 320-327.

[15]. R. Mansour, S.Y. Maziar, R.R. Mohammad and S.R.T. Seyed (2010). The effect of production method on Fe-TiC composite. *Int. J. Min. Process*, 94, pp. 97-100.

[16]. R.H. Md, Z. Hussain and R. Sivakumar (2014). Mechanism and optimization of titanium carbide-reinforced iron composite formation through carbothermal reduction of hematite and anatase. *J. Alloys Compd*, 587, pp. 442-450.

[17]. S.W. Hu, Y.G. Zhao, Z. Wang, Y.G. Li and Q.C. Jiang (2013). Fabrication of in situ TiC locally reinforced manganese steel matrix composite via combustion synthesis during casting. *Mater. Des*, 44, pp. 340-345.

[18]. T.T. Jing and F.C. Zhang (1997). The work-hardening behavior of medium manganese steel under impact abrasive wear condition. *Mater. Lett*, 31, pp. 275-279.

[19]. T. Z. Kattamis and T. Suganuma (1990). Solidification Processing and Tribological Behavior of Particulate TiC Ferrous Matrix CompositesSolidification Processing and Tribological. *MaterialsScience and Engineering*, A128, pp. 241-252.

[20]. W.F. Zhang, X.H. Zhang, J.L. Wang and C.Q. Hong (2004). Effect of Fe on the phases and microstructure of TiC-Fe cermets by combustion synthesis/quasi-isostatic pressing. *Mater. Sci. Eng*, A381, pp. 92-97.

[21]. X. Chen, W. Xiong, Z. Yao, G. Zhang, S. Chen and Q. Yang (2014). Characterization of Tibased solid solution cermets prepared by mechanically induced selfsustained reaction and subsequent pressureless sintering. *J. Alloys Compd*, 583, pp. 523-529.

[22]. Y. Yang, H. Wang, R. Zhao, Y. Liang, L. Zhan and Q. Jiang (2008). Effects of C particle size on the ignition and combustion characteristics of the SHS reaction in the 20 wt%Ni-Ti-C system. *J. Alloys Compd*, 460, pp. 276-282.

[23]. Zhi Wang, Tao Lin, Xinbo He, Huiping Shao, Jianshu Zheng and Xuanhui Qu (2015). Microstructure and properties of TiC-high manganese steel cermet prepared by different sintering processes. *Journal of Alloys and Compounds*, 650, pp. 918-924.